Requirement for and polarized localization of integrin proteins during *Drosophila* wound closure

Si-Hyoung Park[a], Chan-wool Lee[a], Ji-Hyun Lee[a], Jin Young Park[a], Mobina Roshandell[b], Catherine A. Brennan[b], and Kwang-Min Choe[a,*]

[a]Department of Systems Biology, Yonsei University, Seodaemun-gu, Seoul 03722, South Korea; [b]Department of Biological Science, California State University, Fullerton, Fullerton, CA 92831

ABSTRACT **Wound reepithelialization is an evolutionarily conserved process in which skin cells migrate as sheets to heal the breach and is critical to prevent infection but impaired in chronic wounds. Integrin heterodimers mediate attachment between epithelia and underlying extracellular matrix and also act in large signaling complexes. The complexity of the mammalian wound environment and evident redundancy among integrins has impeded determination of their specific contributions to reepithelialization. Taking advantage of the genetic tools and smaller number of integrins in *Drosophila*, we undertook a systematic in vivo analysis of integrin requirements in the reepithelialization of skin wounds in the larva. We identify αPS2-βPS and αPS3-βPS as the crucial integrin dimers and talin as the only integrin adhesion component required for reepithelialization. The integrins rapidly accumulate in a JNK-dependent manner in a few rows of cells surrounding a wound. Intriguingly, the integrins localize to the distal margin in these cells, instead of the frontal or lamellipodial distribution expected for proteins providing traction and recruit nonmuscle myosin II to the same location. These findings indicate that signaling roles of integrins may be important for epithelial polarization around wounds and lay the groundwork for using *Drosophila* to better understand integrin contributions to reepithelialization.**

Monitoring Editor
Richard Fehon
University of Chicago

Received: Nov 17, 2017
Revised: Jun 19, 2018
Accepted: Jul 5, 2018

INTRODUCTION

A skin wound exposes underlying tissues and the entire organism to further damage and infection and so must be healed quickly. "Reepithelialization" (RE), where sheets of skin cells migrate toward and reseal the wound, is a critical part of wound healing. Our knowledge of RE mechanisms is informed by studies of migratory single cells that must polarize, generating functionally different front and rear sides, as well as engage contractile mechanisms to exert force. Finally, controlled adhesion and deadhesion enable movement across a substratum, typically the ECM. Small GTPases of the Rho family mediate front/rear polarization (Ridley *et al.*, 2003; Charest and Firtel, 2007; Parsons *et al.*, 2010), and actomyosin supplies propulsive forces, with actin polymerization driving lamellipodia extension (Vicente-Manzanares *et al.*, 2009; Parsons *et al.*, 2010). Integrins are the major receptors for the extracellular matrix (ECM) and are essential for cell crawling (Scales and Parsons, 2011; Maartens and Brown, 2015). Extensive but poorly understood mutual regulation among the Rho-GTPases, actomyosin, and integrins directs the forward migration of cells (Ridley *et al.*, 2003; Gupton and Waterman-Storer, 2006; Parsons *et al.*, 2010).

Cells migrating as sheets employ similar polarization, contractile, and ECM adhesion mechanisms but must additionally coordinate these across multiple cell diameters and integrate adhesion to both substratum and adjacent cells (Friedl *et al.*, 2014; Collins and Nelson, 2015; Das *et al.*, 2015; Haeger *et al.*, 2015; Ladoux *et al.*, 2016; Mayor and Etienne-Manneville, 2016). In wound healing, further complexity is added by the transient dedifferentiation of epithelial cells to a motile phenotype (Haensel and Dai, 2018),

This article was published online ahead of print in MBoC in Press (http://www.molbiolcell.org/cgi/doi/10.1091/mbc.E17-11-0635) on July 11, 2018.

*Address correspondence to: Kwang-Min Choe (kmchoe@yonsei.ac.kr).

Abbreviations used: ECM, extracellular matrix; JNK, c-Jun N-terminal kinase; RE, reepithelialization; RNAi, RNA interference; WT, wild type.

the regulated mobilization of cells within several rows of the wound (Farooqui and Fenteany, 2005; Matsubayashi *et al.*, 2011; Richardson *et al.*, 2016), the need for the migrating epithelium to remodel the underlying ECM (DiPersio *et al.*, 1997; Nguyen *et al.*, 2000; Longmate *et al.*, 2014), and the inflammatory environment (Gurtner *et al.*, 2008; Shaw and Martin, 2009; Eming *et al.*, 2017).

The physiological complexity of wound healing indicates that the widely employed in vitro scratch wound assays (Boyko *et al.*, 2017) should be supplemented by in vivo studies. *Drosophila* is a valuable model for the genetic analysis of wound healing, as it has been studied at several developmental stages (Kiehart *et al.*, 2000; Wood *et al.*, 2002; Galko and Krasnow, 2004; Munoz-Soriano *et al.*, 2014). Fly epidermal cells are analogous to mammalian keratinocytes in their developmental specification, secretion of protective stratum corneum/cuticle, and regulation after wounding (Mace *et al.*, 2005; Ting *et al.*, 2005; Munoz-Soriano *et al.*, 2014). In both mammals and flies, cells in a restricted number of rows surrounding a wound polarize and, influenced by growth factor ligands from the wound, migrate as a sheet to heal the wound (Barrientos *et al.*, 2008; Wu *et al.*, 2009). Extensive ECM remodeling during wound repair also occurs in both (Stevens and Page-McCaw, 2012; Xue and Jackson, 2015).

Especially important in RE are the integrins, heterodimers of α and β transmembrane glycoproteins that bind the ECM. Integrins nucleate large cytoplasmic complexes that not only tune adhesion in response to both intracellular and extracellular cues (Horton *et al.*, 2015; Iwamoto and Calderwood, 2015) but also engage in bidirectional signaling, affecting cytoskeletal activities and gene expression inside the cell (Legate *et al.*, 2009), and shaping ECM composition on the outside (deHart *et al.*, 2003; Humphrey *et al.*, 2014). Integrin abundance and function are also regulated by transcriptional modulation (Homsy *et al.*, 2006), switching of different integrins (Truong and Danen, 2009; Elosegui-Artola *et al.*, 2014), protein clustering and localization (Yamaguchi *et al.*, 2015), vesicle trafficking (Paul *et al.*, 2015), and protein turnover (Webb *et al.*, 2002; Lopez-Ceballos *et al.*, 2016). Mammals have 18 α and eight β integrins, with extensive combinatorial diversity (Hynes, 2002), and their importance in wound healing is underscored by changes in expression (Grinnell, 1992; Gailit *et al.*, 1994), wound repair defects in animals with integrin-deficient keratinocytes (Grose *et al.*, 2002; Russell *et al.*, 2003; Egles *et al.*, 2010; DiPersio *et al.*, 2016), and the integrin dysregulation seen in human scarring disorders (Wang *et al.*, 2006). The wound phenotypes of many mouse keratinocyte integrin knockouts suggest some functional redundancy, which along with the complexity of the mammalian wound environment has hindered the determination of which adhesion, sensing, and signaling activities of which integrins effect the polarization and traction needed for RE (Margadant *et al.*, 2010; Martins-Green, 2013; DiPersio *et al.*, 2016).

While integrin roles in fly wound repair have not been emphasized, a conserved function is indicated by the induction of integrins in epithelial cells surrounding the wound (Lee *et al.*, 2017) and embryonic wound closure defects in *αPS3* mutants (Campos *et al.*, 2010). Both integrins and their ECM ligands are conserved between flies and mammals (Broadie *et al.*, 2011), but the much smaller number of fly integrins greatly facilitates genetic analysis (Bokel and Brown, 2002). The availability of reagents for the tissue-specific knockdown of any gene in *Drosophila*, including in multiples, is particularly conducive to the study of integrins, which operate in multiple tissues during wound repair, function as heterodimers, and frequently exhibit redundancy. Therefore, we undertook to develop *Drosophila* as a model to study integrin function in wound RE and report here our systematic analysis of the epithelial requirements for specific α and β integrins and core adhesion components in wound closure, the pathways regulating their accumulation, and their contributions to cell polarization.

RESULTS AND DISCUSSION

αPS2/βPS and αPS3/βPS integrin dimers both contribute to epithelial wound closure

To examine integrin involvement in wound healing RE, we knocked down α and β integrins by expressing *UAS-RNAi* transgenes in the larval epidermis using *A58-GAL4* (Galko and Krasnow, 2004). For each gene, we tested nonoverlapping RNA interference (RNAi) lines to exclude off-target effects (Mohr and Perrimon, 2012) and coexpressed *Dicer-2* when necessary to enhance knockdown efficiency (Dietzl *et al.*, 2007). We used a pinch-wound protocol that creates a hole in the epidermis ~30–40 cells wide but leaves the overlying cuticle intact, thus minimizing mortality from hemolymph leakage (Kwon *et al.*, 2010). As we and others have found, such wounds are closed within hours by RE (Galko and Krasnow, 2004; Lee *et al.*, 2017) (Figure 1, A and B).

Epidermal knockdown of *βPS* (*myospheroid*) caused severe RE defects, with 100% or 87% of the wounds still open after 16 h, depending on the RNAi line (Figure 1, C and O, and Supplemental Figure 1A). By 40 h, 0% or 75% of the wounds in *βPS* knockdown larvae had closed, in a delayed manner (Figure 1, D and O, and Supplemental Figure S1B). Wound measurements 20 min after injury in wild-type (WT) vs. *βPS* knockdown larvae found no significant difference in size (Supplemental Figure S2). In further support for a model whereby slowed wound healing in *βPS*-deficient epithelia is due to delayed RE rather than excessive wound sizes, we observed that *βPS*-deficient epithelia failed to display the dynamic shape changes around the wound that normally accompany RE (Figure 1, B–D).

Immunostaining confirmed efficient knockdown of *βPS* (Figure 1, I and J, and Supplemental Figure S1C). Homozygotes for null alleles of the other β-integrin, *βv*, are viable and displayed normal wound closure (Figure 1O and Supplemental Figure S1D), indicating βPS is the only β subunit required for RE.

To identify the αPS subunit(s) that dimerize with βPS integrin in wound closure, we knocked down *αPS1* (*mew*), *2* (*if*), and *3* (*scab*) in the epidermis, but none of these caused defects, with wounds closing efficiently by 14–15 h (Figure 1O and Supplemental Figure S1, E–J). Immunostaining detected no αPS1 in the WT epidermis, consistent with the lack of knockdown phenotype (data not shown). Expression of *αPS1-RNAi* in the wing disk phenocopied the wing blisters of null mutants (unpublished data; Brower and Jaffe, 1989), indicating the *αPS1* RNAi constructs were functional. Anti-αPS2 and anti-αPS3 antibodies detected the corresponding proteins primarily in the plasma membrane of epidermal cells (Figure 1, K and M); in the knockdown larvae, expression levels were severely reduced (Figure 1, L and N, and Supplemental Figure S1, L and M). Altogether, these results indicate that the lack of phenotype was not due to knockdown failure.

We then examined double knockdowns for the three αPS genes. Of the three different combinations, only the *αPS2-αPS3* RNAi pair showed defects, with 96%–82% of the larvae displaying open wounds at 14 h after wounding, (Figure 1, E–H and O, and Supplemental Figure S1K). This reveals that PS2 and PS3 integrins do function in larval epidermal wound closure but may compensate for each other. This is reminiscent of the contemporaneous but distinct roles that αPS2 and αPS3 play in glial cell migration and axon guidance (Tavares *et al.*, 2015).

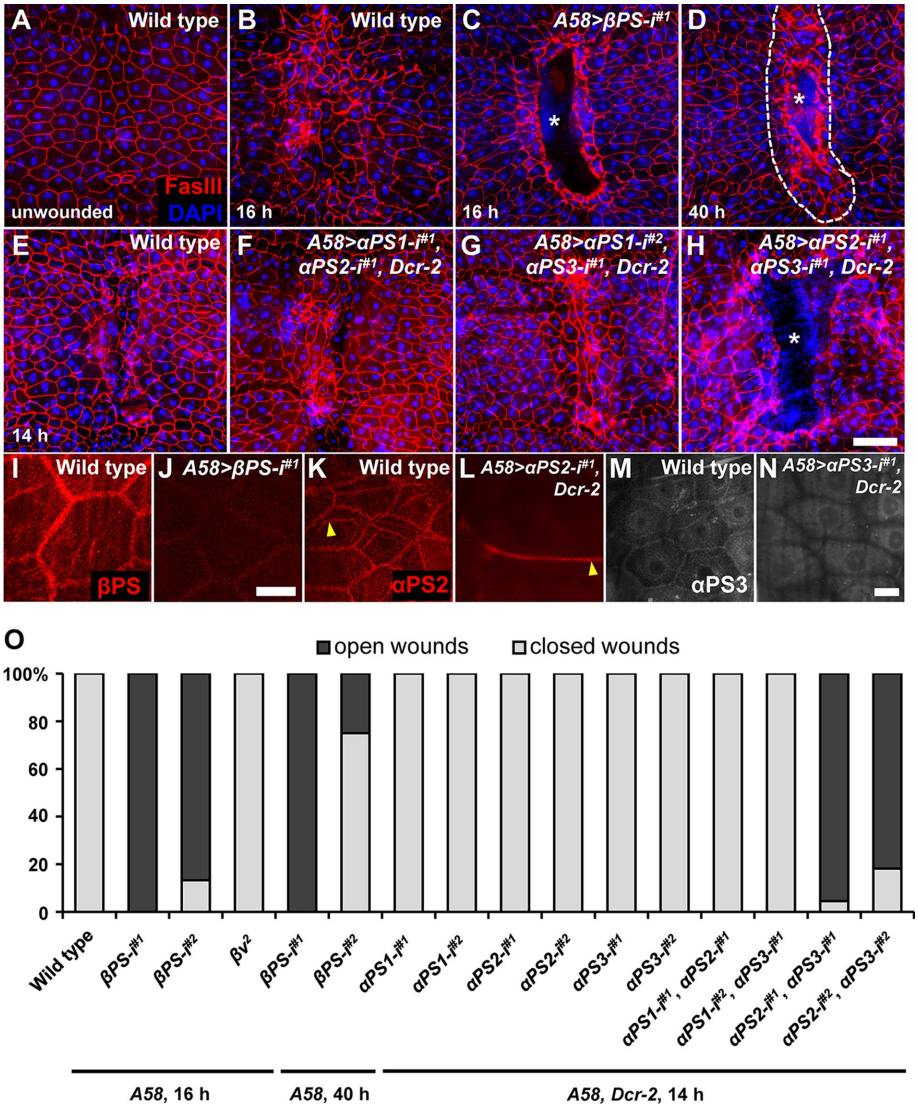

FIGURE 1: Integrins βPS, αPS2, and αPS3 contribute to epithelial wound closure. (A–H) Wound closure was examined in the epidermis of late third instar larvae. Cell boundaries were visualized by FasIII immunostaining in red, and cell nuclei were marked by DAPI staining in blue. (A, B) *A58-GAL4*-only controls, unwounded (A), and dissected at 16 h after wounding (B). (C, D) *A58-GAL4 UAS-βPS RNA-i*$^{\#1}$ (*βPS* knockdown in the larval epidermis of third instar larvae, denoted *A58>βPS-i*$^{\#1}$, hereafter) at 16 h (C) or 40 h (D) after wounding. Asterisks indicate the wound hole. Dashed line indicates the original wound margin. (E–H) Epidermis was dissected at 14 h after wounding. (E) *A58>Dcr-2* only control. (F) *A58>αPS1-i*$^{\#1}$, *αPS2-i*$^{\#1}$, *Dcr-2*. (G) *A58>αPS1-i*$^{\#2}$, *αPS3-i*$^{\#1}$, *Dcr-2*. (H) *A58>αPS2-i*$^{\#1}$, *αPS3-i*$^{\#1}$, *Dcr-2*. Scale bar: 100 μm (A–H). (I–N) Knockdown efficiencies were analyzed by immunostaining in *RNAi*-expressing larvae using anti-βPS (I, J), anti-αPS2 (K, L), and anti-αPS3 (M, N) antibodies in *A58*-only control (I, K, M), *A58>βPS-i*$^{\#1}$ (J), *A58>αPS2-i*$^{\#1}$, *Dcr-2* (L), and *A58>αPS3-i*$^{\#1}$, *Dcr-2* (N) larvae. Yellow arrowheads indicate trachea. Scale bar: 25 μm (I–N). (O) Quantification of the wound closure defects in the larvae of indicated genotypes. At least six animals were analyzed for each genotype.

Talin is required for wound closure, unlike other integrin adhesion components

Integrins function in complexes such as focal adhesions composed of over 50 different proteins (Horton *et al.*, 2015), so we tested 12 of the core complex members. RNAi knockdown of *talin* caused wound closure defects as severe as the *βPS* defects, with 100% of the wounds still open at 16 h (Figure 2, A and B, and Supplemental Figure S1, N–P).

In contrast, knockdown of 11 other integrin complex members failed to cause RE defects, with 100% wound closure at 16 h in all larvae examined. In most cases, we tested multiple RNAi lines, as well as coexpressed *Dicer-2* to increase efficiency, but in no case observed a wound closure defect (Figure 2B). To further validate the knockdown efficiency, we drove each of the *UAS-RNAi* lines using *hs-GAL4* and performed quantitative real-time PCR on the whole larvae. The results indicate that we had at least one RNAi line for each gene that caused greater than 70% reduction in expression, except in the case of *Fak*, *CalpB*, *CalpC*, and *p130CAS* (Figure 2C).

A lack of mutant phenotypes for core integrin components has been observed in many *Drosophila* tissues (Alatortsev *et al.*, 1997; Grabbe *et al.*, 2004; Bulgakova *et al.*, 2012; Moreira *et al.*, 2013; Maartens *et al.*, 2016) and suggests that a robust integrin adhesion structure exists in which components can substitute for each other (Bulgakova *et al.*, 2012). However, the requirement for PINCH and integrin-linked kinase (ILK) in maintaining integrity of the unwounded epidermis (Wang *et al.*, 2015) suggests that the requirement for individual integrin adhesion components is context dependent. In keeping with this idea, even structural domains within adhesome proteins have context-dependent requirements (Ellis *et al.*, 2011). Talin, however, is an indispensable component of integrin adhesions, in both *Drosophila* and mammals, necessary for virtually all adhesion and bidirectional signaling functions of integrins (Brown *et al.*, 2002; Klapholz and Brown, 2017).

Induction and subcellular localizations of α and β integrins after wounding

We recently reported wound induction of βPS integrin in the *Drosophila* epidermis (Lee *et al.*, 2017) and so sought to characterize this expression more thoroughly. βPS expression was markedly increased in the first four rows of cells surrounding the wound margin (Figure 3, A and B), with expression at 7 h post wounding induced 3.1-fold in the first row, 2.4-fold in the second row, and 1.6-fold in the fourth row (Figure 4C). Increased βPS expression lasted past wound closure at 16 h (Figure 3C). Quantitative real-time PCR (qRT-PCR) analysis indicates that at least some of the increased βPS abundance is due to transcriptional up-regulation, although we cannot rule out other mechanisms such as protein stability (Figure 4D). The accumulation of integrin in cells several rows from the wound is consistent with an important role for such "follower cells" in driving sheet migration toward the wound (Farooqui and Fenteany, 2005; Trepat *et al.*, 2009; Matsubayashi *et al.*, 2011; Richardson *et al.*, 2016). Close examination revealed an enrichment of βPS protein at

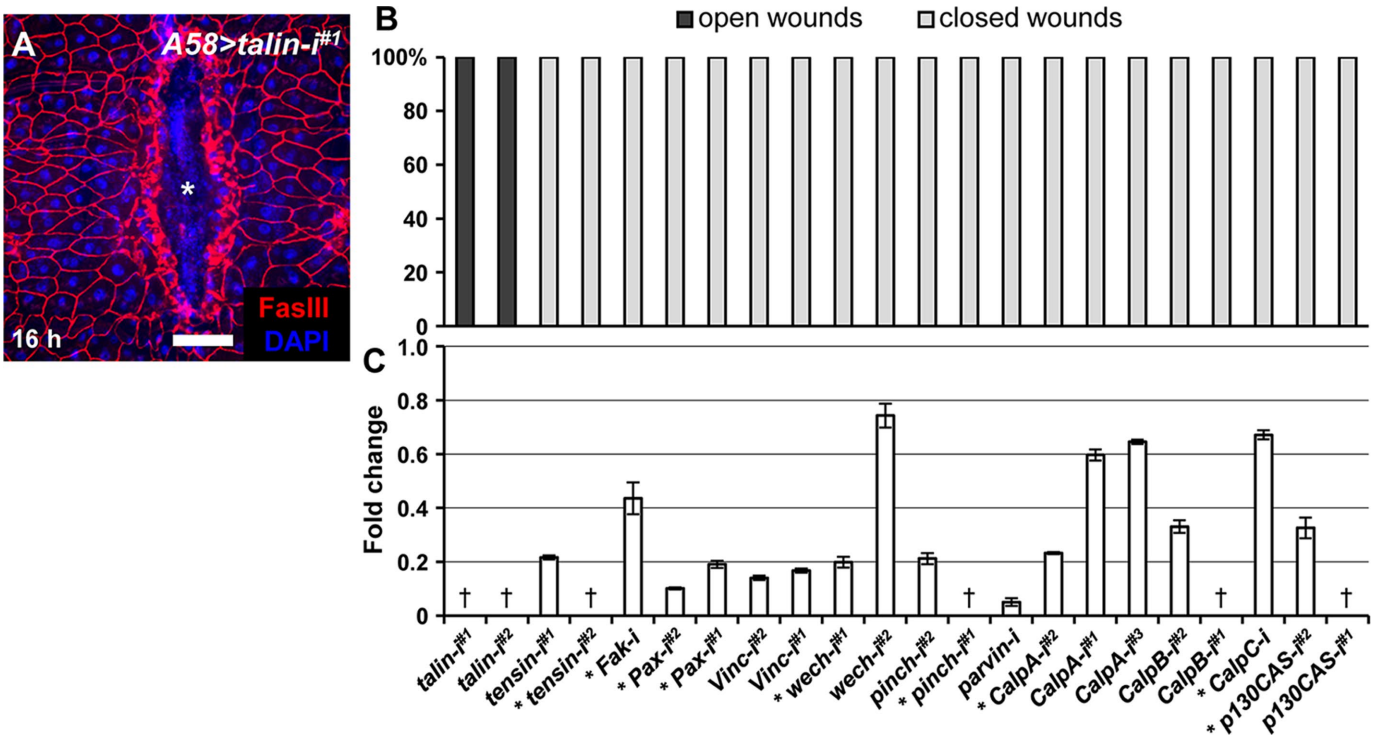

FIGURE 2: Talin is required for efficient wound closure, unlike other components and regulators of integrin-containing adhesive structures. Analysis of wound closure in the epidermis of late third instar larvae at 16 h. (A) *A58>talin-i*$^{\#1}$. Cell boundaries were visualized by FasIII immunostaining in red, and cell nuclei were marked by DAPI staining in blue. Asterisk indicates the wound hole. Scale bar: 100 μm. (B) Quantification of the wound closure defects at 16 h in epithelial RNAi knockdowns of 12 genes encoding components and regulators of integrin adhesive complexes. Asterisks indicate the cases where *UAS-Dcr-2* was added to *A58-GAL4* to enhance knockdown efficiency. For each genotype, at least six wounded animals were analyzed. (C) Analysis of the knockdown efficiency of each *UAS-RNAi* transgene using *hs-GAL4* and qRT-PCR. Cross symbols indicate not tested (for *talin*, see Supplemental Figure S1, O and P; for *pinch*, see Wang *et al.*, 2015). Error bars represent standard errors of the mean.

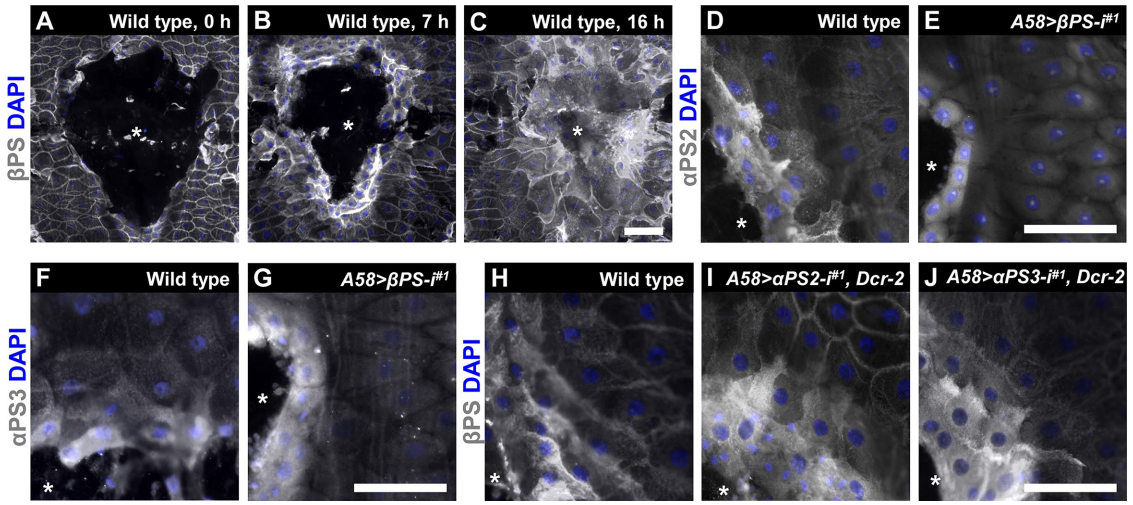

FIGURE 3: Induction and interdependence of α- and β-interins after wounding. Analysis of βPS, αPS2, and αPS3 induction on wounding via immunostaining using anti-βPS (A–C, H–J), anti-αPS2 (D, E), and anti-αPS3 (F, G) antibodies, respectively. Cell nuclei were marked by DAPI staining in blue. Asterisks indicate the wound hole. (A–C) βPS expression in *A58*-only controls at 0 h (A), 7 h (B), and 16 h (C) after wounding, respectively. (D, E) High-magnification images of αPS2 induction at 7 h in cells surrounding a wound in *A58*-only controls (D) and *A58>βPS-i* $^{\#1}$ (E). (F and G) αPS3 induction at 7 h in cells surrounding a wound in *A58*-only controls (F) and *A58>βPS-i*$^{\#1}$ (G). (H–J) βPS induction at 7 h in cells surrounding a wound in *A58*-only controls (H), *A58>αPS2-i* $^{\#1}$, *Dcr-2* (I), and *A58>αPS3-i* $^{\#1}$, *Dcr-2* (J). Scale bar: 100 μm (A-J).

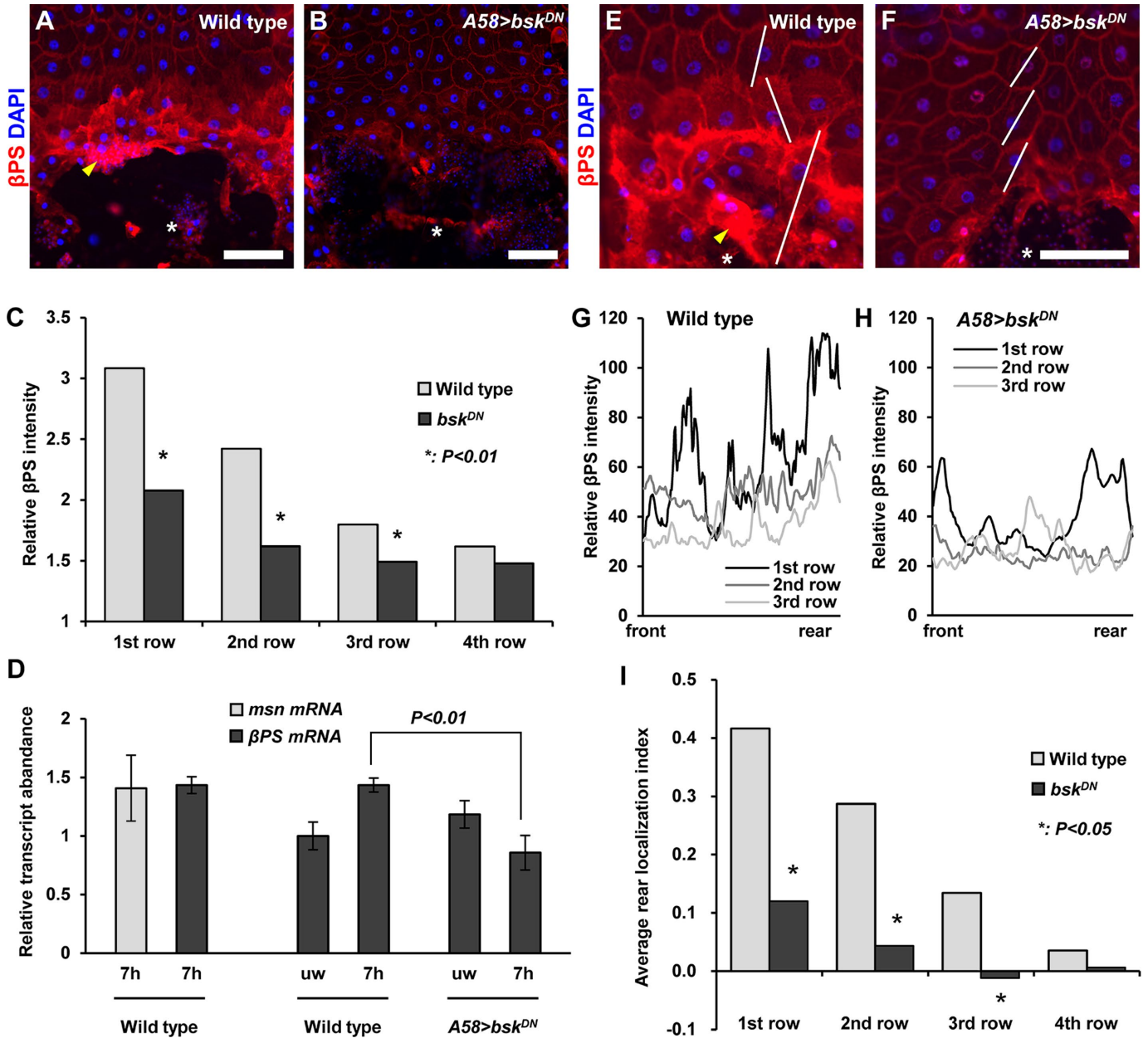

FIGURE 4: JNK-dependent induction and distal localization of βPS integrin in cells surrounding wound. (A, B, E, F) Analysis of βPS induction (A, B) and distal localization (E, F) via immunostaining using anti-βPS antibody in red at 7 h after wounding in *A58*-only controls (A, E) and *A58>bsk*^{DN} (B, F) larvae. Cell nuclei were marked by DAPI staining in blue, and asterisks indicate the wound hole but not necessarily the wound center. Yellow arrowheads indicate occasional strong staining in cell debris at the wound edge. These regions were excluded in measurement, as they did not reflect gene expression in living cells. Scale bar: 100 μm. (C) Quantification of the fluorescence intensities of βPS immunostaining in each of the first four rows of cells from the wound margin in WT vs. JNK-deficient epithelia. (D) qRT-PCR quantification of fold transcriptional induction of *βPS* gene in epithelial fillets at 7 h after wounding. In the first two bars, the *βPS* induction level at 7 h was compared with that of *msn*, which is also induced prominently in the first three to four rows of cells from the wound margin (qRT-PCRs were performed using RNAs prepared from the same epidermal fillets). In the remaining four bars, *βPS* mRNA expression in *A58*-only controls was compared with that in *A58>bsk*^{DN} at 7 h after wounding. Error bars represent standard errors of the mean. (G, H) Plotting of the fluorescence intensities of βPS immunostaining along the front-to-rear axes of individual cells, as marked in white lines in E and F. (I) Quantitative comparison of βPS protein localization in each row of cells between *A58*-only control and *A58>bsk*^{DN} larvae using a "rear localization index." See *Materials and Methods* for the statistical analysis in C and I.

the distal edge of cells surrounding the wound, as has been seen (Figure 3, B and H) (Stevens and Page-McCaw, 2012).

Both the α-integrins that contribute to wound closure were also induced by wounding, although this increased expression was in a narrower band of cells than βPS, approximately two rows around the wound (Figure 3, D and F). Notably, αPS2 had a polarized expression pattern similar to βPS, including enrichment in posterior protrusions (Figure 3D).

We then tested the dependence of the α and β subunits on each other for expression and localization. *βPS* knockdown drastically reduced the plasma membrane localizations of αPS2 and αPS3 (Figure 3, E and G). For αPS2, wound induction of the protein expression was also greatly reduced (Figure 3E). In contrast, levels of βPS induction were normal when either *αPS2* or *αPS3* were singly knocked down, which we attribute to the redundancy of these two α-integrins in wound RE (Figure 3, H–J). Interestingly, the distal accumulation of βPS was impaired in *αPS2* but not *αPS3* knockdowns (Figure 3, H–J). In summary, although wound closure phenotypes were only observed in double knockdowns of *αPS2* and *αPS3*, suggesting some functional redundancy, αPS2 colocalizes with βPS at the posterior of cells surrounding the wound more than does αPS3 and shares a mutual dependency on βPS for this colocalization, possibly indicating a more important role for αPS2 than for αPS3 in βPS dimers in the epidermal wound response.

αPS2/βPS dimers are homologous to mammalian α5β1, α8β1, and αVβ1 (Bokel and Brown, 2002; Johnson *et al*., 2009). Although αPS3 does not have clear mammal orthologues, it most resembles mammal α4 and α9, and like αPS2 is predicted to bind RGD-containing ligands such as laminin and collagen (Johnson *et al*., 2009). Most of these β1-containing integrin dimers are implicated in mammalian wound healing (Koivisto *et al*., 2014; DiPersio *et al*., 2016). It is not clear whether flies, like mammals, deposit a provisional matrix on the wound bed that is different in composition from the unwounded ECM (Barker and Engler, 2017), but increased synthesis of collagen and deposition of matrix is apparent in fly wounds, and surrounding epithelia migrate over both this and cellular debris (Galko and Krasnow, 2004; Stevens and Page-McCaw, 2012). Notably, the distal accumulation of integrin we observed is opposite to the localization in lamellipodia adhesions at the front of singly migrating cells (Scales and Parsons, 2011).

The JNK pathway is required for the polarized accumulation of βPS integrin around the wound

We next sought to characterize the pathway(s) mediating the induction of integrin and its localization to the distal edges of cells around the wound. The Jun N-terminal kinase (JNK) pathway is activated in a gradient extending away from *Drosophila* wounds, downstream of Rho-family small GTPases (Ramet *et al*., 2002; Galko and Krasnow, 2004; Baek *et al*., 2010). Since JNK hyperactivation in unwounded epidermis upregulated βPS integrin (Wang *et al*., 2015), we asked whether JNK is required for the wound induction of βPS. Epithelial expression of a dominant negative allele of the JNK-encoding gene *bsk* (bsk^{DN}) that blocks JNK signaling (Wu *et al*., 2009) greatly reduced βPS accumulation (Figure 4, A–C). Similarly, qRT-PCR analysis in the epithelium revealed JNK contributes to *βPS* transcriptional induction (Figure 4D).

It appeared that the reduced βPS accumulation in JNK-deficient epithelia was also accompanied by a loss of the polarized distribution of βPS around the wound. To quantify this, we assessed polarized βPS localization with a "rear localization index" (see *Materials and Methods*). In WT, the values were 0.42 and 0.29 in the first and second rows of cells surrounding the wound, compared with 0.12 and 0.04 in the corresponding cells in bsk^{DN}-expressing epithelia (Figure 4, E–I). While this supported a role for JNK in generating the polarized accumulation of βPS, it remained possible that the apparent loss of polarized distribution was merely an artifact of the overall reduced βPS expression level. However, when we used RNAi conditions that partially reduce βPS levels, close to the level seen in the bsk^{DN} epithelia (Supplemental Figure S3B vs. Figure 3B), polarized βPS distribution was still apparent, with only a slight, and not statistically significant, decline in rear localization, analyzed in the first and second rows of cells (Supplemental Figure S3E). Our findings thus indicate that in addition to promoting βPS accumulation, JNK signaling may additionally contribute to the polarized distribution of βPS around the wound.

Since integrins are suggested to regulate JNK through Rho-family GTPases (Schwartz and Shattil, 2000; Homsy *et al*., 2006; Matthews *et al*., 2006; Pereira *et al*., 2011; DiPersio *et al*., 2016), we then tested whether integrin function is reciprocally required for JNK pathway activation by wounding but found that knockdown of *βPS* or *talin* did not impair the wound induction of *msn-lacZ*, a JNK pathway reporter (Supplemental Figure S4). Interestingly, in both fly epithelia and cultured cells, loss of integrin adhesions activates JNK (Pereira *et al*., 2011; Wang *et al*., 2015), suggesting that integrin regulation of JNK during wound healing warrants further investigation.

Our data add to the diverse roles of JNK in wound healing in *Drosophila*, which include cytoskeletal reorganization and cell shape changes (Galko and Krasnow, 2004; Bosch *et al*., 2005; Pearson *et al*., 2009; Campos *et al*., 2010; Kwon *et al*., 2010), transcriptional induction of many genes (Pearson *et al*., 2009; Lesch *et al*., 2010; Brock *et al*., 2012; Stevens and Page-McCaw, 2012; Alvarez-Fernandez *et al*., 2015), cytoprotection of neuronal tissues (Nam *et al*., 2012), cell death-induced regeneration (Bergantinos *et al*., 2010), inhibition of polyploidization (Losick *et al*., 2016), cell fusion (Lee *et al*., 2017), and distal accumulation of nonmuscle myosin II (Kwon *et al*., 2010), to include mediating induction and possibly polarized accumulation of integrins. Requirement for the JNK pathway has also been extensively documented in developmental epithelial sheet movements in *Drosophila* (Xia and Karin, 2004), and the few investigations into JNK in vertebrate wound healing are consistent with an evolutionarily conserved RE role (Yates and Rayner, 2002; Li *et al*., 2003; Schafer and Werner, 2007; Richardson *et al*., 2016).

β-Integrin is required for the correct distally polarized accumulation of myosin II in cells surrounding the wound

JNK is required downstream of Rho small GTPases for distal localization of nonmuscle myosin II Zip protein in wounded epidermis (Baek *et al*., 2010), so we analyzed the regulatory relationships between βPS and myosin II. Knockdown of βPS impaired the normal accumulation of a GFP-Zip/myosin II fusion protein after wounding; instead of clustering in arcs along the distal membranes as seen in WT, in *βPS* knockdown cells, GFP-Zip either displayed a polarized membrane accumulation that was somewhat randomized relative to the wound location or failed to localize at the membrane (Figure 5, A and B). For example, in the first row of cells, 62% of *βPS*-depleted cells displayed normal accumulation of myosin II, 32% displayed an incorrectly polarized membrane accumulation, and 6% displayed no membrane accumulation, contrasted with 92% of the WT cells around the wound that exhibited the typical distal recruitment of myosin (Figure 5D). A similar apparent randomized polarization of membrane recruitment of myosin II was observed after wounding in cells knocked down for *talin* gene expression (Figure 5C).

We note that the defects in myosin II accumulation after wounding in *βPS* or *talin* knockdown cells are distinct from those in which JNK signaling is impaired, where myosin II remains cytoplasmic (Kwon *et al*., 2010). This suggests that JNK signaling promotes the membrane accumulation of myosin II after wounding, possibly directing a polarized accumulation. β-integrin, on the other hand, is required to impart the correct directionality to this polarized recruitment of myosin II.

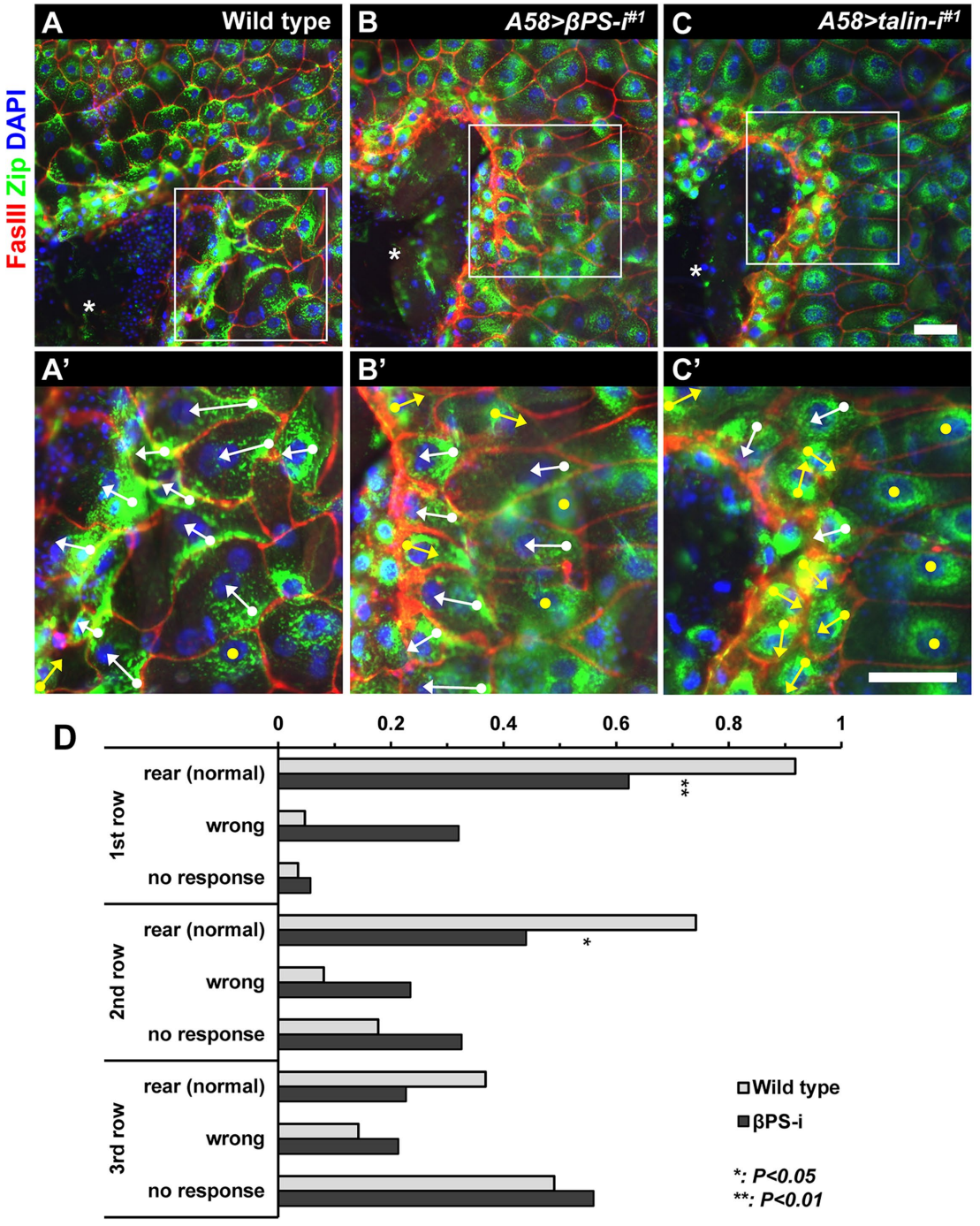

FIGURE 5: βPS is required for rear localization of nonmuscle myosin II during wound closure. Localization of the nonmuscle myosin II heavy chain was examined using GFP-Zip in green at 7 h after wounding. (A, A') *A58*-only. (B, B') *A58>βPS-i*$^{\#1}$. (C, C') *A58>talin-i*$^{\#1}$. (A'–C') Enlarged view of the areas marked in white lines in A–C. Cell boundaries were visualized by FasIII immunostaining in red, and the cell nuclei were marked by DAPI staining in blue. Arrows represent the directionality of individual cells assessed by rear localization of GFP-Zip protein. White arrows indicate a normal direction, and yellow arrows indicate the wrong directions. Yellow dots indicate no response. Asterisks indicate the wound hole. Scale bar: 100 μm. (D) Quantification of the results in A–C, analyzing nonmuscle myosin localization in each of the first three rows of cells from the wound margin. See *Materials and Methods* for the statistical analysis.

Functions of integrins in reepithelialization

In summary, we report that αPS2/βPS and αPS3/βPS dimers are required in the fly larval epidermis for RE following wounding, that talin appears alone among integrin adhesion components to be required for this process, that the induction of integrins following wounding requires JNK, and that integrin accumulates at the distal margin of cells surrounding the wound, where it is required for the similar localization of nonmuscle myosin.

Integrins contribute to wound RE in mammals and fish, but their specific molecular contributions have often been elusive (DiPersio *et al.*, 2016). Our findings offer some clues. While the obvious role for integrins would be adhering to the ECM to provide traction for the migrating epithelium, our findings suggest that this may not be the only, or even the primary, role. Traction for RE that is contributed by cells several rows from the wound is thought to be via "cryptic lamellipodia" (Farooqui and Fenteany, 2005; Trepat *et al.*, 2009; Matsubayashi *et al.*, 2011; Richardson *et al.*, 2016), which is hard to imagine being effected from the distal margin of surrounding cells. The posterior enrichment of integrin in cells surrounding the wound that we and others (Stevens and Page-McCaw, 2012) observed may reflect a role in monitoring the extracellular environment. The ECM undergoes marked changes in tension and composition following wounding, including through the initial rupture, and then through the deposition of replacement components, as well as the action of stiffening enzymes (Kobayashi *et al.*, 1994; Alatortsev *et al.*, 1997; Stramer *et al.*, 2008; Wong *et al.*, 2012; Barker and Engler, 2017). A role for integrins in sensing chemical and mechanical ECM features is well established in cell culture and beginning to be appreciated in wound repair (Kenny and Connelly, 2015; DiPersio *et al.*, 2016).

Possibly relevant to understanding the molecular function of integrins in RE is our finding that talin, but not other "core components," are required for wound healing. Different adhesion components are required for different subfunctions of integrin complexes (Stutchbury *et al.*, 2017), with talin, in particular, implicated in sensing function of adhesions (Kumar *et al.*, 2016; Yao *et al.*, 2016; Rahikainen *et al.*, 2017). Our findings do not preclude an adhesion role for integrins in RE which seems inescapable; it could be that the structural components mediating the adhesive role are somewhat interchangeable (Bulgakova *et al.*, 2012).

The requirement we found for integrin in mediating the distal localization of myosin could simply reflect a localized recruitment of myosin to adhesions, as has been seen (Gupton and Waterman-Storer, 2006; Choi *et al.*, 2008; Vicente-Manzanares *et al.*, 2009). Alternatively, the integrin dependence of distal myosin accumulation might represent a primary role for integrin in polarizing cells relative to the wound; Rho-family GTPase-dependent front-rear polarization of cells by integrins has been well documented (Etienne-Manneville and Hall, 2001; Ridley *et al.*, 2003; Frank and Carter, 2004; Choma *et al.*, 2007) and could be consistent with a sensing role for integrins.

Clearly, there is much yet to learn about integrin contributions to wound healing. The small number of integrin dimers needed for RE in the fly, coupled with the array of genetic tools available, suggest that studies in *Drosophila* may point the way forward.

MATERIALS AND METHODS

Fly strains and genetics

The following lines were obtained from the Bloomington Stock Center: *UAS-bsk^{DN}*, *UAS-Dcr-2*, *msn-lacZ*, and *UAS-Calpain-B-i* [BL25963 (denoted as #2 in superscript)]. The following lines were obtained from the Vienna Drosophila Resource Center (for the strains with numerical-only IDs) or the National Institute of Genetics in Japan (for the strains with IDs containing "R"): *UAS-βPS-i* [1560R-1 (#1), 29619 (#2), and 8070R-1 (#3)], *UAS-talin-i* [6831R-1 (#1) and 40399 (#2)], *UAS-αPS1-i* [1771R-1 (#1) and 44890 (#2)], *UAS-αPS2-i* [100770 (#1) and 44885 (#2)], *UAS-αPS3-i* [4891 (#1) and 100949 (#2)], *UAS-Calpain-A-i* [101294 (#1), 18152R-1 (#2), and 7563R-3 (#3)], *UAS-Calpain-B-i* [23037 (#1)], *UAS-Calpain-C-i* (107844), *UAS-Fak-i* (108608), *UAS-Paxillin-i* [31794R-C-1 (#1) and 107789 (#2)], *UAS-parvin-i* (105356), *UAS-PINCH-i* [7954R-1 (#1) and 100582 (#2)], *UAS-P130CAS-i* [1212R-3 (#1) and 41479 (#2)], *UAS-tensin-i* [9379R-3 (#1) and 22823 (#2)], *UAS-Vinculin-i* [3299R-2 (#1) and 34586 (#2)], and *UAS-wech-i* [1642R-2 (#1) and 106390 (#2)]. The following lines were obtained from private collections: *A58-GAL4* (M. Galko, MD Anderson Cancer Center), *UAS-GFP-Zip* (D. Kiehart, Duke University), and $\beta\nu^2$ (Y. Nakanishi, Kanazawa University, Japan).

Wounding, immunohistochemistry, and β-galactosidase staining

For epidermal wounding, third instar larvae were pinched at the dorsal side using a pair of forceps (Fine Science Tools, Cat. No. 11295-00). A wound with the typical size of 30–40 cells was generated in the abdominal segment A3-A4 (Kwon *et al.*, 2010). Larvae were allowed some time for recovery in food and were pinned down at their heads and tails on a silicon plate for dissection. Each larva was immersed in several drops of phosphate-buffered saline (PBS), and the outer integuments were torn open on the ventral side. Internal organs were removed, and the remaining epidermal fillet was spread wide using four more pins at the rectangular corners. In some cases, muscles were carefully removed by forceps for a better result in immunostaining. The tissue was fixed in 4% paraformaldehyde for 30 min, and the remaining fixative was washed out using PBS twice.

For immunohistochemistry, a fixed sample was first incubated in a primary antibody plus 2% normal goat serum in PBS supplemented with 0.2% Triton X-100 (PBST) overnight at 4°C. The sample was then incubated in a secondary antibody plus 0.2% PBST for 2 h at room temperature. For nuclear staining, 4′,6-diamidino-2-phenylindole (DAPI) was used at 0.01 μg/ml. Washed samples were mounted in 80% glycerol or Vectashield (Vector Laborartories, Cat. No. H-1200) and subjected to fluorescent microscopy (Olympus BX40 and Zeiss Imager.A2, with AxioCamMRc5) or confocal imaging (Zeiss LSM 510 META). Anti-FasIII (1:100, 7G10), anti-βPS (1:50, CF6G11), anti-αPS1 (1:50, DK.1A4), anti-αPS2 (1:10, CF.2C7), and anti-Talin (1:100, A22A or E16B) were obtained from the Developmental Studies Hybridoma Bank. Chicken anti–β-galactosidase antibody (1:1000, ab9361) was purchased from Abcam. Anti-αPS3 (1:100) and anti-Talin (1:100) were gifts from S. Hayashi (Riken Center for Developmental Biology, Japan) and N. Brown (University of Cambridge, UK), respectively. Cy3-conjugated goat anti-mouse immunoglobulin G (IgG) (1:200, 115-165-003) was purchased from the Jackson ImmunoResearch. Alexa 488-conjugated goat anti-mouse IgG (1:200; A-11001), goat anti-rat IgG (1:200; A-11006), and goat anti-rabbit IgG (1:200; A-11008) and Alexa 546-conjugated goat anti-chicken IgG (1:200; A-11040), goat anti-mouse IgG (1:200; A-11003), and goat anti-rabbit IgG (1:200; A-11035) were all purchased from Invitrogen (ThermoFisher Scientific). For analysis, some images are stitched using "pairwise stitching" plugin of Fiji (ImageJ2) (Preibisch *et al.*, 2009).

For β-galactosidase staining, dissected samples were fixed in 2% glutaraldehyde for 15 min at room temperature. The samples were washed with PBS two times and incubated in 10 mM $NaPO_4$, 150 mM NaCl, 1 mM $MgCl_2$, 3.1 mM $K_4[Fe_{II}(CN)_6]$, 3.1 mM $K_3[Fe_{III}(CN)_6]$, 0.3% Triton X-100, and 0.2% X-Gal for 2 h at 37°C.

Quantitative real-time PCR

Total RNA was extracted using Trizol from 15 epidermal fillets in Figure 4D or from 20 to 30 whole larvae in Figure 2C in triplicates for each experimental condition. For the heat shock condition in Figure 2C, larvae were given a heat shock at 37°C for 30 min at 72 h after egg laying, incubated at 25°C for 24 h, and given another heat shock for 30 min, incubated at 25°C for 24 h, and then lysed. cDNAs were synthesized from 2 μg RNA using Moloney murine leukemia virus reverse transcriptase (M-MLV RT) (Promega, Cat. No. M1701).

Quantitative real-time PCR was performed using SYBR Premix Ex Taq (Tli RNaseH Plus; Takara, Cat. No. RR420A) and each of the values was normalized by the corresponding value of *rp49*. Relative mRNA levels were calculated using the comparative cycle threshold (Ct) method. The following primers were used: 5′-CAGTCGGATCGATATGCTAAGCTGT-3′ and 5′-TAACCGATGTTGGGCATCAGATACT-3′ for *rp49*; 5′-CCTGGCTAAAGTCGAAGATCTTG-3′ and 5′-GTTCCGACGCTCCACTTGAT-3′ for *msn*; 5′-TGGCGAGTGTCACTTGAGTC-3′ and 5′-CAACCACATTGGATGAATCG-3′ for *mys*; 5′-AGGAGACCGTTTTCCATGTG-3′ and 5′-AGTGCTTCTAGCCAGCCAAA-3′ for *Fak*; 5′-CATCCACATCGACATCCAAG-3′ and 5′-GCTGTTGGCCATTGGTATTT-3′ for *tensin*; 5′-TAACGGATCTGCGCATAAAT-3′ and 5′-GCCATCAGATCATCCAGTTC-3′ for *Pax*; 5′-ACCCGATTGGCTAAGGAGTT-3′ and 5′-ACGGTGGACAGGATTTTCAG-3′ for *Vinc*; 5′-CGAGCGTCTCCAGTGTTAAT-3′ and 5′-AGCTATTGTCTCGCAACAGG-3′ for *wech*; 5′-TTGAGGAGAGGGTGGTAACG-3′ and 5′-ACATCGCCTCCAATA ACCTG-3′ for *pinch*; 5′-CACCAAAAGATTCCCA AGTG-3′ and 5′-TCGTCGTACTCGGACGTTAT-3′ for *parvin*; 5′-AAATCGTCAGG GAAAGATCC-3′ and 5′-GCGATCGAAGTGGTTAAGAA-3′ for *CalpA*; 5′-GCTGGCATCTTTCACTTCAA-3′ and 5′-TAAGATCCATGCAGCT TTGC-3′ for *CalpB*; 5′-GAAGCGTATCATGGA TTTGG-3′ and 5′-CA CCACGCGATAGAAGAGAT-3′ for *CalpC*; 5′-CTGA TCTTAGGCAGCAACCA-3′ and 5′-AAGTCGTAGGTCAGCC CACT-3′ for *p130CAS*.

Quantification of βPS protein induction

For quantification of anti-βPS immunofluorescence, Fiji (ImageJ2) was used. Immunohistochemical micrographs for βPS were converted to eight-bit images, and cells were sorted into different rows manually using Selection and XOR tools: cells (excluding cell debris) located immediately adjacent to the wound margin were designated to the first row category, and cells in the next row to the second row category, and so on. The value of fluorescence intensity per area (V_1) was read for each of the rows using the Measure tool. The value for the noninduced state (V_2) was obtained using the Threshold and Creative Selection tools by selecting cells in the neighboring segment adjacent to the wounded segment, or in some occasions, cells in the same wounded segment but located farthest away and were still polygonal in shape (Kwon *et al.*, 2010). Last, the value of the background (V_0) was determined by reading fluorescence intensities of cell-free regions and was used for background subtraction. The fold increase of βPS protein in a specific row was then calculated as $V = (V_1\text{-}V_0)/(V_2\text{-}V_0)$. Eight WT and six bsk^{DN} animals were analyzed. For statistical analysis in Figure 4C, Mann–Whitney *U* test was used. Rank sum values of the first to fourth rows of WT samples were 38, 36, 39, and 48, and those of bsk^{DN} samples were 67, 69, 66, and 57, respectively. The *p* values of two-sided test of each row were 0.0045, 0.0019, 0.0067, and 0.1213.

Quantification of the rear localization of βPS

A line was drawn along the frontal-rear axis of a cell in the wounded area, and the intensity value of anti-βPS immunofluorescence was obtained along the axis using ImageJ2. Owing to the large size and nonsymmetrical shape of a typical wound hole, the exact determination of the frontal-rear axis was sometimes arbitrary. We, however, tried to take the longest line that passes over the nucleus and lies within the degree of ±45° from the wound center. The rear localization index was calculated in the following way: the intensity value of the rear half of the cell minus that of the frontal half of the cell divided by the intensity value of the frontal half of the cell. Five WT and six bsk^{DN} larvae were analyzed, and 19 cells from each row were analyzed on average (that was >70% of the total cells in a row and was essentially all the cells that were analyzable), which was presented in Figure 4I. For statistical analysis, both Student's *t* test and Mann–Whitney *U* test were used. For Student's *t* test, the rear localization index of each cell was regarded as an independent value. The *p* values of two-side test of each row were 4.3×10^{-8}, 6.8×10^{-11}, 2.7×10^{-9}, and 0.214. For Mann–Whitney *U* test, the mean of the rear localization index of each row was calculated and regarded as a value for rank calculation. Rank sum values of the first to fourth rows of the WT samples were 17, 16, 16, and 22, and those of bsk^{DN} were 49, 50, 50, and 44, respectively. The *p* values of the two-sided test of each row were 0.0176, 0.0106, 0.0106, and 0.1441. In Supplemental Figure S3E, five larvae of each of WT and $\beta PS\text{-}i^{\#3}$ were dissected, and 54 cells of WT and 68 cells of $\beta PS\text{-}i^{\#3}$, collectively combined from the first and second rows were analyzed. The *p* values were 0.30 and 0.34 in Student's *t* test and Mann–Whitney *U* test, respectively.

Quantification of GFP-Zip localization

The directionality and polarization of GFP-Zip was measured in the first three rows of cells from the wound margin. A symbol of compass was overlaid on each and every cell within the area using a circle with a "×" mark in the middle to determine the directionality of a cell. The compass was set toward the wound center or set perpendicular to the tangent line of the wound leading edge. If GFP-Zip was polarized in the correct direction, that was within the degree of 90°, then the cell was sorted as "normal." If GFP-Zip was not polarized and remained around the nucleus as if the epidermis was not wounded, then these cells were sorted as "no response." Cells that were ambiguous in directionality or polarization due to tissue damage, cell fusion, or other reasons were carefully excluded from the analysis. For statistical analysis in Figure 5D, Mann–Whitney *U* test was used. Six animals for each of WT and bsk^{DN} were analyzed. Rank sum values of the rear localization index of the first to third rows of the WT samples were 22, 25, and 27, and those of bsk^{DN} were 56, 53, and 51, respectively. The *p* values of two-sided test of each row were 0.0065, 0.025, and 0.0547.

ACKNOWLEDGMENTS

We thank N. Brown, M. Galko, S. Hayashi, D. Kiehart, Y. Nakanishi, The Bloomington Stock Center, The National Institute of Genetics in Japan, and The Vienna Drosophila Resource Center for fly stocks and antibodies. This research was supported by the Basic Science Research Program through the National Research Foundation of Korea funded by the Ministry of Education, Science and Technology (NRF-2015R1A2A2A01006660 and NRF-2018R1D1A1B07048933) to K.-M.C. and by grants from the California State University Program for Education and Research in Biotechnology (CSUPERB) and the National Institutes of Health (SC2AI133653) to C.A.B.

REFERENCES

Alatortsev VE, Kramerova IA, Frolov MV, Lavrov SA, Westphal ED (1997). Vinculin gene is non-essential in Drosophila melanogaster. FEBS Lett 413, 197–201.

Alvarez-Fernandez C, Tamirisa S, Prada F, Chernomoretz A, Podhajcer O, Blanco E, Martin-Blanco E (2015). Identification and functional analysis of healing regulators in Drosophila. PLoS Genet 11, e1004965.

Baek SH, Kwon YC, Lee H, Choe KM (2010). Rho-family small GTPases are required for cell polarization and directional sensing in Drosophila wound healing. Biochem Biophys Res Commun 394, 488–492.

Barker TH, Engler AJ (2017). The provisional matrix: setting the stage for tissue repair outcomes. Matrix Biol 60-61, 1–4.

Barrientos S, Stojadinovic O, Golinko MS, Brem H, Tomic-Canic M (2008). Growth factors and cytokines in wound healing. Wound Repair Regen 16, 585–601.

Bergantinos C, Corominas M, Serras F (2010). Cell death-induced regeneration in wing imaginal discs requires JNK signalling. Development 137, 1169–1179.
Bokel C, Brown NH (2002). Integrins in development: moving on, responding to, and sticking to the extracellular matrix. Dev Cell 3, 311–321.
Bosch M, Serras F, Martin-Blanco E, Baguna J (2005). JNK signaling pathway required for wound healing in regenerating Drosophila wing imaginal discs. Dev Biol 280, 73–86.
Boyko TV, Longaker MT, Yang GP (2017). Laboratory models for the study of normal and pathologic wound healing. Plast Reconstr Surg 139, 654–662.
Broadie K, Baumgartner S, Prokop A (2011). Extracellular matrix and its receptors in Drosophila neural development. Dev Neurobiol 71, 1102–1130.
Brock AR, Wang Y, Berger S, Renkawitz-Pohl R, Han VC, Wu Y, Galko MJ (2012). Transcriptional regulation of Profilin during wound closure in Drosophila larvae. J Cell Sci 125, 5667–5676.
Brower DL, Jaffe SM (1989). Requirement for integrins during Drosophila wing development. Nature 342, 285–287.
Brown NH, Gregory SL, Rickoll WL, Fessler LI, Prout M, White RA, Fristrom JW (2002). Talin is essential for integrin function in Drosophila. Dev Cell 3, 569–579.
Bulgakova NA, Klapholz B, Brown NH (2012). Cell adhesion in Drosophila: versatility of cadherin and integrin complexes during development. Curr Opin Cell Biol 24, 702–712.
Campos I, Geiger JA, Santos AC, Carlos V, Jacinto A (2010). Genetic screen in Drosophila melanogaster uncovers a novel set of genes required for embryonic epithelial repair. Genetics 184, 129–140.
Charest PG, Firtel RA (2007). Big roles for small GTPases in the control of directed cell movement. Biochem J 401, 377–390.
Choi CK, Vicente-Manzanares M, Zareno J, Whitmore LA, Mogilner A, Horwitz AR (2008). Actin and alpha-actinin orchestrate the assembly and maturation of nascent adhesions in a myosin II motor-independent manner. Nat Cell Biol 10, 1039–1050.
Choma DP, Milano V, Pumiglia KM, DiPersio CM (2007). Integrin alpha-3beta1-dependent activation of FAK/Src regulates Rac1-mediated keratinocyte polarization on laminin-5. J Invest Dermatol 127, 31–40.
Collins C, Nelson WJ (2015). Running with neighbors: coordinating cell migration and cell-cell adhesion. Curr Opin Cell Biol 36, 62–70.
Das T, Safferling K, Rausch S, Grabe N, Boehm H, Spatz JP (2015). A molecular mechanotransduction pathway regulates collective migration of epithelial cells. Nat Cell Biol 17, 276–287.
deHart GW, Healy KE, Jones JC (2003). The role of alpha3beta1 integrin in determining the supramolecular organization of laminin-5 in the extracellular matrix of keratinocytes. Exp Cell Res 283, 67–79.
Dietzl G, Chen D, Schnorrer F, Su KC, Barinova Y, Fellner M, Gasser B, Kinsey K, Oppel S, Scheiblauer S, *et al.* (2007). A genome-wide transgenic RNAi library for conditional gene inactivation in Drosophila. Nature 448, 151–156.
DiPersio CM, Hodivala-Dilke KM, Jaenisch R, Kreidberg JA, Hynes RO (1997). alpha3beta1 Integrin is required for normal development of the epidermal basement membrane. J Cell Biol 137, 729–742.
DiPersio CM, Zheng R, Kenney J, Van De Water L (2016). Integrin-mediated regulation of epidermal wound functions. Cell Tissue Res 365, 467–482.
Egles C, Huet HA, Dogan F, Cho S, Dong S, Smith A, Knight EB, McLachlan KR, Garlick JA (2010). Integrin-blocking antibodies delay keratinocyte re-epithelialization in a human three-dimensional wound healing model. PLoS One 5, e10528.
Ellis SJ, Pines M, Fairchild MJ, Tanentzapf G (2011). In vivo functional analysis reveals specific roles for the integrin-binding sites of talin. J Cell Sci 124, 1844–1856.
Elosegui-Artola A, Bazellieres E, Allen MD, Andreu I, Oria R, Sunyer R, Gomm JJ, Marshall JF, Jones JL, Trepat X, Roca-Cusachs P (2014). Rigidity sensing and adaptation through regulation of integrin types. Nat Mater 13, 631–637.
Eming SA, Wynn TA, Martin P (2017). Inflammation and metabolism in tissue repair and regeneration. Science 356, 1026–1030.
Etienne-Manneville S, Hall A (2001). Integrin-mediated activation of Cdc42 controls cell polarity in migrating astrocytes through PKCzeta. Cell 106, 489–498.
Farooqui R, Fenteany G (2005). Multiple rows of cells behind an epithelial wound edge extend cryptic lamellipodia to collectively drive cell-sheet movement. J Cell Sci 118, 51–63.
Frank DE, Carter WG (2004). Laminin 5 deposition regulates keratinocyte polarization and persistent migration. J Cell Sci 117, 1351–1363.
Friedl P, Wolf K, Zegers MM (2014). Rho-directed forces in collective migration. Nat Cell Biol 16, 208–210.
Gailit J, Welch MP, Clark RA (1994). TGF-beta 1 stimulates expression of keratinocyte integrins during re-epithelialization of cutaneous wounds. J Invest Dermatol 103, 221–227.
Galko MJ, Krasnow MA (2004). Cellular and genetic analysis of wound healing in Drosophila larvae. PLoS Biol 2, E239.
Grabbe C, Zervas CG, Hunter T, Brown NH, Palmer RH (2004). Focal adhesion kinase is not required for integrin function or viability in Drosophila. Development 131, 5795–5805.
Grinnell F (1992). Wound repair, keratinocyte activation and integrin modulation. J Cell Sci 101(Pt 1), 1–5.
Grose R, Hutter C, Bloch W, Thorey I, Watt FM, Fassler R, Brakebusch C, Werner S (2002). A crucial role of beta 1 integrins for keratinocyte migration in vitro and during cutaneous wound repair. Development 129, 2303–2315.
Gupton SL, Waterman-Storer CM (2006). Spatiotemporal feedback between actomyosin and focal-adhesion systems optimizes rapid cell migration. Cell 125, 1361–1374.
Gurtner GC, Werner S, Barrandon Y, Longaker MT (2008). Wound repair and regeneration. Nature 453, 314–321.
Haeger A, Wolf K, Zegers MM, Friedl P (2015). Collective cell migration: guidance principles and hierarchies. Trends Cell Biol 25, 556–566.
Haensel D, Dai X (2018). Epithelial-to-mesenchymal transition in cutaneous wound healing: where we are and where we are heading. Dev Dyn 247, 473–480.
Homsy JG, Jasper H, Peralta XG, Wu H, Kiehart DP, Bohmann D (2006). JNK signaling coordinates integrin and actin functions during Drosophila embryogenesis. Dev Dyn 235, 427–434.
Horton ER, Byron A, Askari JA, Ng DHJ, Millon-Fremillon A, Robertson J, Koper EJ, Paul NR, Warwood S, Knight D, *et al.* (2015). Definition of a consensus integrin adhesome and its dynamics during adhesion complex assembly and disassembly. Nat Cell Biol 17, 1577–1587.
Humphrey JD, Dufresne ER, Schwartz MA (2014). Mechanotransduction and extracellular matrix homeostasis. Nat Rev Mol Cell Biol 15, 802–812.
Hynes RO (2002). Integrins: bidirectional, allosteric signaling machines. Cell 110, 673–687.
Iwamoto DV, Calderwood DA (2015). Regulation of integrin-mediated adhesions. Curr Opin Cell Biol 36, 41–47.
Johnson MS, Lu N, Denessiouk K, Heino J, Gullberg D (2009). Integrins during evolution: evolutionary trees and model organisms. Biochim Biophys Acta 1788, 779–789.
Kenny FN, Connelly JT (2015). Integrin-mediated adhesion and mechano-sensing in cutaneous wound healing. Cell Tissue Res 360, 571–582.
Kiehart DP, Galbraith CG, Edwards KA, Rickoll WL, Montague RA (2000). Multiple forces contribute to cell sheet morphogenesis for dorsal closure in Drosophila. J Cell Biol 149, 471–490.
Klapholz B, Brown NH (2017). Talin—the master of integrin adhesions. J Cell Sci 130, 2435–2446.
Kobayashi H, Ishii M, Chanoki M, Yashiro N, Fushida H, Fukai K, Kono T, Hamada T, Wakasaki H, Ooshima A (1994). Immunohistochemical localization of lysyl oxidase in normal human skin. Br J Dermatol 131, 325–330.
Koivisto L, Heino J, Hakkinen L, Larjava H (2014). Integrins in wound healing. Adv Wound Care (New Rochelle) 3, 762–783.
Kumar A, Ouyang M, Van den Dries K, McGhee EJ, Tanaka K, Anderson MD, Groisman A, Goult BT, Anderson KI, Schwartz MA (2016). Talin tension sensor reveals novel features of focal adhesion force transmission and mechanosensitivity. J Cell Biol 213, 371–383.
Kwon YC, Baek SH, Lee H, Choe KM (2010). Nonmuscle myosin II localization is regulated by JNK during Drosophila larval wound healing. Biochem Biophys Res Commun 393, 656–661.
Ladoux B, Mege RM, Trepat X (2016). Front-rear polarization by mechanical cues: from single cells to tissues. Trends Cell Biol 26, 420–433.
Lee JH, Lee CW, Park SH, Choe KM (2017). Spatiotemporal regulation of cell fusion by JNK and JAK/STAT signaling during Drosophila wound healing. J Cell Sci 130, 1917–1928.
Legate KR, Wickstrom SA, Fassler R (2009). Genetic and cell biological analysis of integrin outside-in signaling. Genes Dev 23, 397–418.
Lesch C, Jo J, Wu Y, Fish GS, Galko MJ (2010). A targeted UAS-RNAi screen in Drosophila larvae identifies wound closure genes regulating distinct cellular processes. Genetics 186, 943–957.
Li G, Gustafson-Brown C, Hanks SK, Nason K, Arbeit JM, Pogliano K, Wisdom RM, Johnson RS (2003). c-Jun is essential for organization of the epidermal leading edge. Dev Cell 4, 865–877.

Longmate WM, Monichan R, Chu ML, Tsuda T, Mahoney MG, DiPersio CM (2014). Reduced fibulin-2 contributes to loss of basement membrane integrity and skin blistering in mice lacking integrin alpha3beta1 in the epidermis. J Invest Dermatol 134, 1609–1617.
Lopez-Ceballos P, Herrera-Reyes AD, Coombs D, Tanentzapf G (2016). In vivo regulation of integrin turnover by outside-in activation. J Cell Sci 129, 2912–2924.
Losick VP, Jun AS, Spradling AC (2016). Wound-induced polyploidization: Regulation by hippo and JNK signaling and conservation in mammals. PLoS One 11, e0151251.
Maartens AP, Brown NH (2015). Anchors and signals: the diverse roles of integrins in development. Curr Top Dev Biol 112, 233–272.
Maartens AP, Wellmann J, Wictome E, Klapholz B, Green H, Brown NH (2016). Drosophila vinculin is more harmful when hyperactive than absent, and can circumvent integrin to form adhesion complexes. J Cell Sci 129, 4354–4365.
Mace KA, Pearson JC, McGinnis W (2005). An epidermal barrier wound repair pathway in Drosophila is mediated by grainy head. Science 308, 381–385.
Margadant C, Charafeddine RA, Sonnenberg A (2010). Unique and redundant functions of integrins in the epidermis. FASEB J 24, 4133–4152.
Martins-Green M (2013). The yin and yang of integrin function in re-epithelialization during wound healing. Adv Wound Care (New Rochelle) 2, 75–80.
Matsubayashi Y, Razzell W, Martin P (2011). "White wave" analysis of epithelial scratch wound healing reveals how cells mobilise back from the leading edge in a myosin-II-dependent fashion. J Cell Sci 124, 1017–1021.
Matthews BD, Overby DR, Mannix R, Ingber DE (2006). Cellular adaptation to mechanical stress: role of integrins, Rho, cytoskeletal tension and mechanosensitive ion channels. J Cell Sci 119, 508–518.
Mayor R, Etienne-Manneville S (2016). The front and rear of collective cell migration. Nat Rev Mol Cell Biol 17, 97–109.
Mohr SE, Perrimon N (2012). RNAi screening: new approaches, understandings, and organisms. Wiley Interdiscip Rev RNA 3, 145–158.
Moreira CG, Jacinto A, Prag S (2013). Drosophila integrin adhesion complexes are essential for hemocyte migration in vivo. Biol Open 2, 795–801.
Munoz-Soriano V, Lopez-Domenech S, Paricio N (2014). Why mammalian wound-healing researchers may wish to turn to Drosophila as a model. Exp Dermatol 23, 538–542.
Nam HJ, Jang IH, You H, Lee KA, Lee WJ (2012). Genetic evidence of a redox-dependent systemic wound response via Hayan protease-phenoloxidase system in Drosophila. EMBO J 31, 1253–1265.
Nguyen BP, Ryan MC, Gil SG, Carter WG (2000). Deposition of laminin 5 in epidermal wounds regulates integrin signaling and adhesion. Curr Opin Cell Biol 12, 554–562.
Parsons JT, Horwitz AR, Schwartz MA (2010). Cell adhesion: integrating cytoskeletal dynamics and cellular tension. Nat Rev Mol Cell Biol 11, 633–643.
Paul NR, Jacquemet G, Caswell PT (2015). Endocytic trafficking of integrins in cell migration. Curr Biol 25, R1092–R1105.
Pearson JC, Juarez MT, Kim M, Drivenes O, McGinnis W (2009). Multiple transcription factor codes activate epidermal wound-response genes in Drosophila. Proc Natl Acad Sci USA 106, 2224–2229.
Pereira AM, Tudor C, Kanger JS, Subramaniam V, Martin-Blanco E (2011). Integrin-dependent activation of the JNK signaling pathway by mechanical stress. PLoS One 6, e26182.
Preibisch S, Saalfeld S, Tomancak P (2009). Globally optimal stitching of tiled 3D microscopic image acquisitions. Bioinformatics 25, 1463–1465.
Rahikainen R, von Essen M, Schaefer M, Qi L, Azizi L, Kelly C, Ihalainen TO, Wehrle-Haller B, Bastmeyer M, Huang C, Hytonen VP (2017). Mechanical stability of talin rod controls cell migration and substrate sensing. Sci Rep 7, 3571.
Ramet M, Lanot R, Zachary D, Manfruelli P (2002). JNK signaling pathway is required for efficient wound healing in Drosophila. Dev Biol 241, 145–156.
Richardson R, Metzger M, Knyphausen P, Ramezani T, Slanchev K, Kraus C, Schmelzer E, Hammerschmidt M (2016). Re-epithelialization of cutaneous wounds in adult zebrafish combines mechanisms of wound closure in embryonic and adult mammals. Development 143, 2077–2088.
Ridley AJ, Schwartz MA, Burridge K, Firtel RA, Ginsberg MH, Borisy G, Parsons JT, Horwitz AR (2003). Cell migration: integrating signals from front to back. Science 302, 1704–1709.
Russell AJ, Fincher EF, Millman L, Smith R, Vela V, Waterman EA, Dey CN, Guide S, Weaver VM, Marinkovich MP (2003). Alpha 6 beta 4 integrin regulates keratinocyte chemotaxis through differential GTPase activation and antagonism of alpha 3 beta 1 integrin. J Cell Sci 116, 3543–3556.
Scales TM, Parsons M (2011). Spatial and temporal regulation of integrin signalling during cell migration. Curr Opin Cell Biol 23, 562–568.
Schafer M, Werner S (2007). Transcriptional control of wound repair. Annu Rev Cell Dev Biol 23, 69–92.
Schwartz MA, Shattil SJ (2000). Signaling networks linking integrins and rho family GTPases. Trends Biochem Sci 25, 388–391.
Shaw TJ, Martin P (2009). Wound repair at a glance. J Cell Sci 122, 3209–3213.
Stevens LJ, Page-McCaw A (2012). A secreted MMP is required for reepithelialization during wound healing. Mol Biol Cell 23, 1068–1079.
Stramer B, Winfield M, Shaw T, Millard TH, Woolner S, Martin P (2008). Gene induction following wounding of wild-type versus macrophage-deficient Drosophila embryos. EMBO Rep 9, 465–471.
Stutchbury B, Atherton P, Tsang R, Wang DY, Ballestrem C (2017). Distinct focal adhesion protein modules control different aspects of mechanotransduction. J Cell Sci 130, 1612–1624.
Tavares L, Pereira E, Correia A, Santos MA, Amaral N, Martins T, Relvas JB, Pereira PS (2015). Drosophila PS2 and PS3 integrins play distinct roles in retinal photoreceptors-glia interactions. Glia 63, 1155–1165.
Ting SB, Caddy J, Hislop N, Wilanowski T, Auden A, Zhao LL, Ellis S, Kaur P, Uchida Y, Holleran WM, *et al*. (2005). A homolog of Drosophila grainy head is essential for epidermal integrity in mice. Science 308, 411–413.
Trepat X, Wasserman MR, Angelini TE, Millet E, Weitz DA, Butler JP, Fredberg JJ (2009). Physical forces during collective cell migration. Nat Phys 5:426–430
Truong H, Danen EH (2009). Integrin switching modulates adhesion dynamics and cell migration. Cell Adh Migr 3, 179–181.
Vicente-Manzanares M, Ma X, Adelstein RS, Horwitz AR (2009). Non-muscle myosin II takes centre stage in cell adhesion and migration. Nat Rev Mol Cell Biol 10, 778–790.
Wang Y, Antunes M, Anderson AE, Kadrmas JL, Jacinto A, Galko MJ (2015). Integrin adhesions suppress syncytium formation in the Drosophila larval epidermis. Curr Biol 25, 2215–2227.
Wang Z, Fong KD, Phan TT, Lim IJ, Longaker MT, Yang GP (2006). Increased transcriptional response to mechanical strain in keloid fibroblasts due to increased focal adhesion complex formation. J Cell Physiol 206, 510–517.
Webb DJ, Parsons JT, Horwitz AF (2002). Adhesion assembly, disassembly and turnover in migrating cells—over and over and over again. Nat Cell Biol 4, E97–E100.
Wong VW, Longaker MT, Gurtner GC (2012). Soft tissue mechanotransduction in wound healing and fibrosis. Semin Cell Dev Biol 23, 981–986.
Wood W, Jacinto A, Grose R, Woolner S, Gale J, Wilson C, Martin P (2002). Wound healing recapitulates morphogenesis in Drosophila embryos. Nat Cell Biol 4, 907–912.
Wu Y, Brock AR, Wang Y, Fujitani K, Ueda R, Galko MJ (2009). A blood-borne PDGF/VEGF-like ligand initiates wound-induced epidermal cell migration in Drosophila larvae. Curr Biol 19, 1473–1477.
Xia Y, Karin M (2004). The control of cell motility and epithelial morphogenesis by Jun kinases. Trends Cell Biol 14, 94–101.
Xue M, Jackson CJ (2015). Extracellular matrix reorganization during wound healing and its impact on abnormal scarring. Adv Wound Care (New Rochelle) 4, 119–136.
Yamaguchi N, Mizutani T, Kawabata K, Haga H (2015). Leader cells regulate collective cell migration via Rac activation in the downstream signaling of integrin beta1 and PI3K. Sci Rep 5, 7656.
Yao M, Goult BT, Klapholz B, Hu X, Toseland CP, Guo Y, Cong P, Sheetz MP, Yan J (2016). The mechanical response of talin. Nat Commun 7, 11966.
Yates S, Rayner TE (2002). Transcription factor activation in response to cutaneous injury: role of AP-1 in reepithelialization. Wound Repair Regen 10, 5–15.